Local Earthquake Tomography for Imaging Mining-Induced Changes Within the Overburden above a Longwall Mine

Westman, E.C. and Luxbacher, K.D.
Department of Mining and Minerals Engineering, Virginia Tech, Blacksburg, VA, USA
Swanson, P.L.
National Institute for Occupational Safety and Health-Spokane Research Laboratory, Spokane, WA, USA

ABSTRACT: Three-dimensional velocity tomograms were generated on a daily basis to image mining-induced changes to the overburden above a longwall mine. The hypothesis was that a coherent redistribution of seismic velocity, due to the development of high-stress zones, could be imaged at the mine scale. Seam depth was 360 m and source location depth varied from 100 to 1000 m. Sixteen geophones were distributed over a 600 by 600 m square area on the surface above the mine. More than 12,500 events were recorded over an 18 day period. The recorded seismicity provided input for the local-earthquake tomography code, SIMULPS. Eighteen tomograms were generated and high-velocity regions correlated well with high abutment stresses. Additionally, the high-velocity regions were observed to redistribute as the longwall face retreated. These results indicate that velocity tomography can be used to provide a better understanding of temporal changes within a rock mass, and can potentially be used to produce a better understanding of the mechanisms that lead to unanticipated ground failures.

1. INTRODUCTION

The ability to forecast failure of rock is an ultimate goal of the geo-engineering field. Failure within a rock mass is often a poorly understood phenomenon which can have severe consequences, even where best-design practices are employed. Failure within a rock mass is currently predicted by comparing values of stress and strength based on estimated material properties. Frequently, numerical models are used to represent the rock structure by dividing it into elements and summing the behavior of the elements. Each element relates applied stresses to strains through a constitutive equation. Different material properties can be assigned to various portions of the model. However, the correct estimate of the necessary material properties is a key problem with numerical modeling of rock structures; without accurate estimates of the material properties, the changes induced by loading of a rock mass are inaccurate.

A potential remedy to this problem is to perform high-resolution imaging to monitor the true alteration of a rock mass as it is loaded. Because rock properties change under increased loads, areas of high stress can be identified using elastic waves [1,2,3]. Elastic waves include ultrasonic waves, typically used in the laboratory [4], and seismic waves, common in field studies [5,6,7]. These waves can be used to nondestructively image the interior of rock masses and determine changes to loading of the rock mass [8]. One method used to perform this imaging is tomography, which is a rapidly advancing method for imaging the interior of bodies, including rock masses [9,10,11].

Tomography has been used at the field scale as long ago as 20 years in the mining industry to image geologic features as well as stress-related features [12,13,14]. It was not until the last 15 years, however, that it has had ready acceptance within the geosciences for petroleum reservoir characterization and for geotechnical applications. More recently, the method has been adapted to image stress concentrations ahead of a longwall face by a unique application of the longwall mining equipment as the seismic source [15,16].

The objective of this study was to determine whether a qualitative but coherent redistribution of velocity, indicating change in location of induced stress, could be imaged as mining occurred in known locations by using a local earthquake tomography software code. Local earthquake tomography uses the many naturally-occurring or mining-induced seismic events as sources to both generate a tomographic image of the velocity

distribution within the rock mass and relocate the seismic events.

2.0 BACKGROUND

Tomographic imaging was first described by Radon [17] who theorized that the interior of a body could be imaged by analyzing energy which passed from one boundary to another. This technology was eventually adapted to the medical field [18,19] and to the geosciences [20]. It has been shown in the lab that changing stress concentrations in rock can be imaged with tomography [21-24]. Scott et al. [25,26,27] indented cylindrical rock samples and imaged the sample as stress was increased. The tomograms showed a clear increase in ultrasonic wave velocity directly beneath the load.

Information about the actual deformation processes in the rock mass can be obtained by monitoring the propagation of elastic waves [28-31]. These methods are divided into two groups, passive and active. Passive methods listen to the emissions generated during localized failure within the rock mass, for example microseisms and acoustic emissions [32]. With active methods a signal is generated on one boundary of the sample (e.g. with a hammer blow or explosive charge) and acquired on another, following a pitch-and-catch method [33-36].

Local earthquake tomography is a passive method that has not previously been used specifically for studying mining-related stress redistribution. With this method initial event locations are used to generate a tomogram. This three-dimensional velocity model is an improvement to the initial one-dimensional ("layer cake") model used to initially locate the events, thus the events can be relocated more accurately. The process is iterated until the difference between the measured and calculated travel times is at an acceptable level. The SIMULPS local earthquake tomography code was developed based on Thurber's damped-least squares, full matrix inversion and allows curved rays [37-40].

Hudson [41] lists eleven different terms used to describe stress within a rock mass. Within this paper, the term 'stress' will refer to 'induced stress' in which the natural state of stress has been altered by human activity.

3.0 STUDY SITE

Data for this study were collected between July 7, 1997 and August 8, 1997, at an underground coal mine in the western United States. The mine employs longwall mining, and the coal seam ranges in thickness from 2.6 to 3.0m with a depth of approximately 360m. The operation mines longwall panels that are approximately 5500m long and 250m wide. Over the course of the study, the face advanced 431m, averaging about 24m per day. Sixteen geophones were assembled on the surface to monitor and locate microseismic events. The geophones provided adequate spatial coverage of the entire area of study.

A unique feature of the mining area was that three entries were cut through the panel to provide an alternate escapeway due to the length of the panels. Shortly before mining through, the cross-panel entries were backfilled with light-weight cement. This cement carried only a portion of the induced stress because its stiffness was less than the pillars. The backfilled entries, cross-panel pillars and the panel were instrumented. Analysis of this data showed that nothing unusual occurred as they mined through the backfill [42].

4.0 DATA COLLECTION AND ANALYSIS

Seismic data were collected at the site over an 18 day period. As mining progressed, the void left by removal of the ore created a stress concentration ahead of the mining face, resulting in higher stresses and mining-induced seismicity as the rock failed. An individual seismic event was logged to the database if it triggered at least ten geophones. The events typically had a frequency around 30 Hz. The number of events recorded per day was related to the amount of mining that was done and varied from about 100 to more than 800 events per day, with a mean of 650.

Input for tomography consists of many sets of the combination of receiver location, source location and travel time of the seismic wave between the source and receiver. The receiver locations were surveyed using the same coordinate system as the mine. The source locations were based on an automated arrival time determination and a one-dimensional velocity model, as described in Luxbacher et al. [43].

Several parameters within the SIMULPS program are important to note. The program allowed a grid of voxels 30m on each side. Event locations were adjusted a maximum of 15m per iteration with a maximum of 20 iterations per event to minimize the residual between measured and calculated travel times. A damping value of 500 was selected empirically following the procedure recommended by Evans et al. [37]. Damping values that are too low result in a highly variant, 'noisy' model while too much damping reduces the ability of the model

to fit the data well. The final velocity model was compared to the initial velocity model in MATLAB and the difference plotted using the default trilinear interpolation. A voxel size of 15m was used in MATLAB to smooth the images.

5.0 RESULTS AND DISCUSSION

Six plan-view tomograms at seam level are shown as Figure 1, including the face location and the related mine geometry. Two features are clearly apparent. One is that a high-velocity zone, indicating high stress, extends along the tailgate pillar area. The other is that as the face advances, a parallel high-velocity zone ahead of the face also advances. Figure 1 shows this zone to lose its coherency as the face approaches and passes through the backfilled entries (Figure 1a-d) and is then clearly reestablished in subsequent days (Figure 1e,f).

Results of the study include event relocation as well as the tomograms. Histograms of initial event locations and the relocated events (Figure 2) show that the locations based on the SIMULPS-generated velocity model are closer to the seam, as indicated by the narrowing of the depth distribution. This is as would be expected and is attributed to the improved velocity model used for event location.

There are important parameters that must be clearly understood when applying tomographic methods in the field. The resolution of the tomographic image is a function of several factors. The number of sources and receivers used in the study determines the number of raypaths traversing the body, influencing the resolution of the image. The number of sensors is determined, in part, by the size of the body and the data acquisition system capabilities. The frequency characteristics of the elastic waves also influence the resolution with which features can be identified. Laboratory studies are typically conducted using ultrasonic waves with frequencies near 1 MHz, resulting in wavelengths of approximately 0.4 cm (assuming propagation velocity of 3500 m/s). Large-scale field studies, on the other hand, must use lower frequency waves (typically < 200 Hz) to allow greater propagation distances. These waves in the same material have a wavelength of nearly 18 m. Because features will only be well resolved if they are of diameter greater than one-half the wavelength, the difference in observable features is substantial. Given an average velocity of 3600 m/sec and a typical frequency of 30 Hz, a wavelength of 120 m is typical for the dataset.

Major stress features resulting from abutment stress were expected to be imaged through velocity tomography. Abutment stress is a result of stress redistribution due to the extraction of ore, and occurs along or near the boundary where material has been removed [44]. An undisturbed coal seam with competent roof and floor strata will have a fairly uniform stress distribution. As coal is removed this distribution is disrupted and the load shifts to another intact area. In longwall mining, this stress is transferred immediately in front of the face, and to the sides of the panel (headgate and tailgate). Failure of the roof strata behind the longwall shields is termed the ‘gob’ and allows for pressure relief. Very competent strata above a longwall system, such as massive sandstone, may not cave immediately, contributing to extremely high abutment stress in front of the face which can result in rockbursts at the face, and damage to shields due to dynamic loading [45]. The exact distribution of the abutment load is dependent upon the properties of the roof strata and the mining geometry, but abutment stress is usually the largest on the tailgate, if it is adjacent to a previously mined out panel. Front abutment pressure is detectable at a lateral distance ahead of the face approximately equal to the overburden depth, and typically reaches a maximum at a distance of one-tenth the overburden depth [45]. In addition to vertical stress redistribution, joints, faults, inhomogeneous layering, and horizontal stress orientation may contribute to larger abutment stresses and more erratic failure. Even in optimum conditions roof failure behind longwall shields is rarely uniform [46].

The relationship between induced stress and velocity is not monotonic and is complicated by confinement. In uniaxial compression the velocity of an elastic wave traveling through the sample increases as existing microfractures are closed. At some point on the stress-strain curve new microfractures are formed which eventually coalesce into the failure plane. The point at which these new microfractures begin forming varies with lithology, but is generally between 50 and 90 percent of the ultimate failure strength. As these new microfractures are formed the elastic wave travels more slowly. Few laboratory studies have been conducted to evaluate the effect of confinement, however it is likely that because the ultimate strength of the sample is increased, the stress at which the new microfractures are formed is also increased and the behavior is similar to that of uniaxial compression.

In this study, as the longwall face retreated down the panel, high stress zones were formed where the

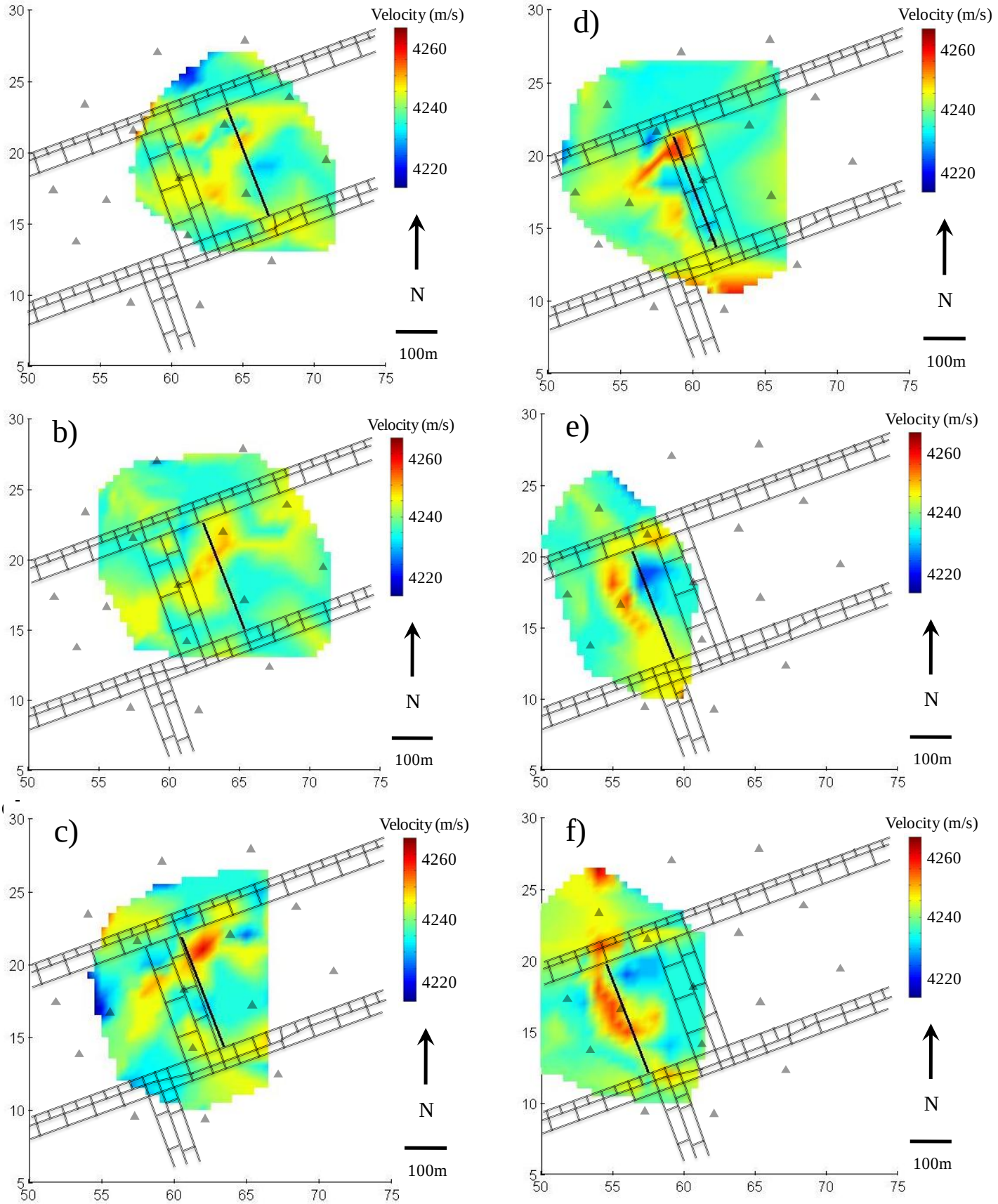

Figure 1. Tomogram near seam level for a) Day 4, b) Day 6, c) Day 8, d) Day 12, e) Day16 and f) Day 18. Geophone locations on earth's surface are shown as filled triangles. The mining face for the given day is denoted by the solid black line. Note that as the face advances, a parallel high-velocity zone ahead of the face also advances. This zone loses its coherency as the face approaches and passes through the backfilled entries (Figure 1a-d) and is then clearly reestablished in subsequent days (Figure 1e,f).

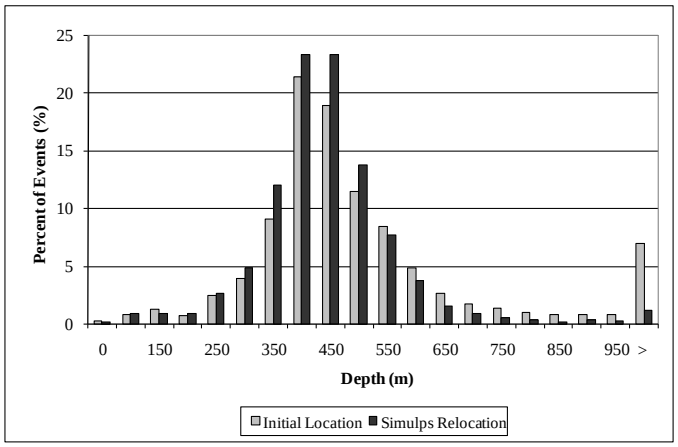

Figure 2. Histogram showing depths of seismic events as initially located and as relocated using SIMULPS. Seam is at a depth of 360 m. Narrowing of the distribution of depths is attributed to the improved velocity model used for event location.

supporting coal was removed. This condition was especially met along the mining face, which had a newly formed void on one side of it, and along the pillars in the tailgate, which had void on either side.

6.0 CONCLUSIONS

Several conclusions can be drawn from this study. The first is that local earthquake tomography can be used to generate a reasonable, coherent redistribution of velocity indicative of and correlated with, stress redistribution due to mining. Even with the sub-optimal arrangement of receivers located only on the earth's surface well above mining-induced seismicity, a high-velocity zone was consistently shown to move with the mining face. This high velocity feature indicates the location of the forward abutment stress which moves with the face.

The second conclusion is that improved seismic event locations are obtained through the use of local earthquake tomography. Initially, the events were located based on a velocity model that increased monotonically with depth, but did not vary laterally. By generating a more accurate velocity model the events were relocated closer to the seam that was being mined.

Several improvements can be made in the future. The data set would be improved by including sensors at the seam level and also by daily observation of conditions at the mining face. Future research must also include correlating a tomogram to seismic energy generated at a subsequent time, with the goal being a tool for forecasting regions of elevated seismic activity. The ultimate goal for the mining engineering community is the increased safety of underground miners.

ACKNOWLEDGEMENTS

The authors are grateful to the National Institute for Occupational Safety and Health for providing the raw data for this study. This research was funded by a National Science Foundation CAREER Grant (CMS-0134034).

REFERENCES

1. Friedel, M.J., R.E. Thill, 1990, Stress determination in rock using the Kaiser effect, USBM RI 9286, 20 pp.

2. Su, W.H., S.S. Peng, 1986, Development of analytical model for prediction of in-situ stresses from in-mine p-wave velocity measurements, Dept. of Mining Engineering, West Virginia University, January.

3. Su, W.H., S.S. Peng, S. Okubo, K. Matsuki, 1983, Development of ultrasonic methods for measuring in-situ stresses at great depth, *Mining Science and Technology*, vol. 1, pp. 21-42.

4. Allison, H., R.D. Lama, 1979, Low frequency sounding technique for predicting progressive failure of rock, *Rock Mechanics*, vol. 12, pp. 79-97.

5. By, T.L., 1986, Acoustic monitoring of in situ static deformation modulus at a dam site, *Norwegian Geotechnical Institute*, vol.164, 5 pp.,

6. Gladwin, M.T., 1982, Ultrasonic stress monitoring in underground mining, *Int. J. Rock Mech. Min. Sci. & Geomech. Abstr.*, vol 19, pp. 221-228.

7. Gochioco, L.M., 1990, Seismic surveys for coal exploration and mine planning, *Geophysics: The Leading Edge of Exploration*, pp. 25-28.

8. Scott, T.E., Q. Ma, J.C. Roegiers, Z. Reches, 1994, Dynamic stress mapping utilizing ultrasonic tomography, *Rock Mechanics Models and Measurements Challenges from Industry*, Nelson & Laubach, pp. 427-434.

9. Chow, M.T., I.L. Meglis, R.P. Young, 1995, Progressive microcrack development in tests on Lac du Bonnet Granite; II, Ultrasonic tomographic imaging, *Int. J. Rock Mech. Min. Sci. & Geomech. Abstr.*,, vol. 32, no. 8, pp. 751-761.

10. Debski, W., R.P. Young, 1999, Enhanced velocity tomography; practical method of combining velocity and attenuation parameters, *Geophysical Research Letters*, vol. 26, no. 21, pp. 3253-3256.

11. Terada, M., T. Yanagidani, 1986, Application of ultrasonic computer tomography to rock mechanics, *Ultrasonic Spectroscopy and its applications to materials science*, pp. 205-210.

12. Buchanan, D.J., R. Davis, P.J. Jackson, P.M. Taylor, 1981, Fault location by channel wave seismology in United Kingdom coal seams, *Geophysics*, vol. 46, pp. 1065-1073.

13. Kormendi, A., T. Bodoky, L. Hermann, L. Dianiska, T. Kalman, 1986, Seismic measurements for safety in mines, *Geophysical Prospecting*, vol. 34, pp. 1022-1037.

14. Mason, I.M., 1981, Algebraic Reconstruction of a two-dimensional velocity inhomogeneity in the High Hazles Seam of Thoresby Colliery, *Geophysics*, vol. 46, pp. 298-308.

15. Westman, E.C., K.Y. Haramy, A.D. Rock, 1996, Seismic tomography for longwall stress analysis, *Rock Mechanics Tools and Techniques*, Aubertin, Hassani & Mitri, pp. 397-403.

16. Westman, E.C., K.A. Heasley, P.L. Swanson, S. Paterson, 2001, A correlation between seismic tomography, seismic events and support pressure, *Proc. 38th Rock Mech. Symp*, Washington DC, July 7-10, pp. 319-326.

17. Radon, J., 1917, Uber die bestimmung von functionen durch ihre integralwere lange gewisser mannigfaltigkeiten, *Ber. Verh. Saechs. Akad. Wiss.*, vol. 69, pp. 262-267.

18. Cormack, A.M., 1973, Reconstruction of densities from their projections, with applications in radiological physics, *Phys. Med. Biol*, vol. 18, no. 2, pp. 195-207.

19. Hounsfield, G.N., 1973, Computerized transverse axial scanning (tomography). 1. description of system, *Br. J. Radiol.*, vol.46, no. 552, pp. 1016-1022.

20. Dines, K.A., and J.R. Lytle, 1979, Computerized geophysical tomography, *Proc. IEEE*, vol. 67, no. 7, pp. 1065-1073.

21. Maxwell, S.C., R..P. Young, 1995, A controlled in-situ investigation of the relationship between stress, velocity and induced seismicity, *Geophysical Research Letters*, vol. 22, no. 9, pp. 1049-1052.

22. Maxwell, S.C., R. P. Young, 1996, Seismic Imaging of Rock Mass Responses to Excavation, *Int. J. Rock Mech. Min. Sci. & Geomech. Abstr.*, vol 33, no. 7, pp. 713-724.

23. Seya, K., I. Suzuki, H Fujiwara, 1979, The Change in Ultrasonic Wave Velocities in Triaxially Stressed Brittle Rock, *J. Phys. Earth*, vol. 27, pp. 409-421.

24. Shea-Albin, R.V., D.R. Hanson, R.E. Gerlick, 1991,Elastic Wave Velocity and Attenuation as Used to Define Phases of Loading and Failure in Coal, USBM RI 9355, 43 pp.

25. Scott, T.E., Q. Ma, J.C. Roegiers, 1994, Ultrasonic tomographic imaging of compaction in limestones, *Eos, Transactions, American Geophysical Union*, vol. 75, no. 44, pp. 638.

26. Scott, T.E., Q. Ma, J.C. Roegiers, Z. Reches, 1994, Acoustic tomographic difference imaging of dynamic stress fields, SPE/ISRM International Conference, Delft, Netherlands, Aug. 29-31, pp. 99-104.

27. Scott, T.E., Q. Ma, J.C. Roegiers, Z. Reches, 1993, Tomographic acoustic velocity changes induced during indentation of Berea Sandstone, *Eos, Transactions, American Geophysical Union*, vol. 74, no. 43, pp. 408.

28. Bieniawski, Z.T., 1978, Determining rock mass deformability: experience from case histories, *Int. J. Rock Mech. Min. Sci. & Geomech. Abstr.*, vol 15, pp. 237-247.

29. Carlson, S.R., R..P. Young, 1993, Acoustic emission and ultrasonic velocity study of excavation-induced microcrack damage at the Underground Research Laboratory, *Int. J. Rock Mech. Min. Sci. & Geomech. Abstr.*,, vol. 30, no. 7, pp. 901-907.

30. Falls, S.D., R.P. Young, 1998, Acoustic emission and ultrasonic-velocity methods used to characterise the excavation disturbance associated with deep tunnels in hard rock, *Tectonophysics*, vol. 289, pp. 1-15.

31. Scott, T.E., M.M. Zaman, J.C. Roegiers, 1998, Acoustic-velocity signatures associated with rock-deformation processes, *Journal of Petroleum Technology*, vol. 50, no. 6, pp. 70-72.

32. Jansen, D.P., R.S. Carlson, R. P. Young, 1993, Ultrasonic imaging and acoustic emission monitoring of thermally induced microcracks in Lac du Bonnet Granite, *Journal of Geophysical Research, B, Solid Earth and Planets*, vol. 98, no. 12, pp. 22, 231-22, 243.

33. Bieniawski, Z.T., 1978, The 'petite sismique' technique – a review of current developments, *2nd Conf. on Acoustic Emission/Microseismic Activity in Geologic Structures and Materials – Penn State Univ*., Nov. 13-15, pp. 305-318.

34. Molina, J.P., B. Wack, 1982, Crack field characterization, *Int. J. Rock Mech. Min. Sci. & Geomech. Abstr.*, vol. 19, pp. 267-278.

35. Sjogren, B., A. Ofsthus, J. Sandberg, 1979, Seismic classification of rock mass qualities, *Geophysical Prospecting*, vol. 27, no. 2, June, pp. 409-442.

36. Thill, R.E., 1973, Acoustic methods for monitoring failure in rock, *Proceedings-14th Symposium on Rock Mechanics*, vol. 14, pp. 649-687.

37. Evans J. R., D. Eberhart-Phillips, and C.H. Thurber, 1994, User's manual for SIMULPS12 for imaging Vp and Vp/Vs: A derivative of the Thurber tomographic inversion SIMUL3 for local earthquakes and explosions, USGS-OFR-94-431, 101 pp.

38. Thurber, C. H., 1993, Local earthquake tomography: velocities and Vp/Vs - theory,in Seismic Tomography: Theory and Practice, edited by H. M. Iyer and K. Hirahara.

39. Eberhart-Phillips,D, 1993, Local earthquake tomography: earthquake source regions, in Seismic Tomography: Theory and Practice, edited by H. M. Iyer and K. Hirahara.

40. Thurber, C. H., 1983, Earthquake locations and three-dimensional crustal structure in the Coyote Lake area, central California, J. Geophys. Res., v. 88, p. 8226-8236.

41. Hudson, J. A, 2003, Strategy and tactics for rock stress estimation, in Rock Stress, edited by K. Sugawara, Y. Obara, and A. Sato, pp. 3-21.

42. Seymour et al. 1998, Stability of backfilled cross-panel entries during longwall mining, *Proc. of the 17th International Conference Ground Control in Mining*, Morgantown, WV.

43. Luxbacher, M.K., P.I. Swanson, M.K. Karfakis and E.C. Westman, 3-D, time lapse tomograms over a longwall coal mine, *Int. J. Rock Mech. Min. Sci. & Geomech. Abstr.*,, Jun 2008,Vol 45, pp. 478-485.

44. Peng SS, and H.S. Chiang, 1983, *Longwall mining*, New York: Wiley.

45. Haramy KY, J.A. Magers, J.P. McDonnell, 1988, Mining under strong roof, *Proc. of the 7th International Conference Ground Control in Mining*, Morgantown, WV, p. 179–94.

46. Maleki H. 2002, The application of geotechnical monitoring to stability evaluation and mine design, *Proc. of Society for Mining Metallurgy and Exploration annual meeting*, Phoenix.